Available online at www.sciencedirect.com

ScienceDirect

Procedia Structural Integrity 2 (2016) 072–079

Structural Integrity Procedia

www.elsevier.com/locate/procedia

21st European Conference on Fracture, ECF21, 20-24 June 2016, Catania, Italy

An elastic-interface model for the mixed-mode bending test under cyclic loads

Stefano Bennati[a], Paolo Fisicaro[a], Paolo S. Valvo[a]*

[a]*University of Pisa, Department of Civil and Industrial Engineering, Largo Lucio Lazzarino, 56122 Pisa, Italy*

Abstract

We have developed a mechanical model of the mixed-mode bending (MMB) test, whereby the specimen is considered as an assemblage of two identical sublaminates, modelled as Timoshenko beams. The sublaminates are partly connected by a linearly elastic–brittle interface, transmitting stresses along both the normal and tangential directions with respect to the interface plane. The model is described by a set of suitable differential equations and boundary conditions. Based on the explicit solution of this problem and following an approach already adopted to model buckling-driven delamination growth in fatigue, we analyse the response of the MMB test specimen under cyclic loads. Exploiting the available analytical solution, we apply a fracture mode-dependent fatigue growth law. As a result, the number of cycles needed for a delamination to extend to a given length can be predicted.

Peer-review under responsibility of the Scientific Committee of PCF 2016.

Keywords: Composite laminate; delamination; fatigue; mixed-mode bending test; beam theory; elastic interface.

1. Introduction

Composite laminates generally present strongly orthotropic fracture properties under both quasi-static and cyclic loads. Several experimental procedures and testing setups have been developed to determine the delamination toughness and to study fatigue behaviour of laminated specimens under pure and mixed fracture modes. Bak et al. (2014) have reviewed the available experimental observations, phenomenological models and computational simulation methods for delamination growth under fatigue loads in composite laminates.

* Corresponding author. Tel.: +39-050-2218223; fax: +39-050-2218201.
E-mail address: p.valvo@ing.unipi.it

Peer review under responsibility of the Scientific Committee of PCF 2016.
10.1016/j.prostr.2016.06.010

The *mixed-mode bending* (MMB) test is used to characterise pre-cracked fibre-reinforced composite laminates under I/II mixed-mode fracture conditions. Within the context of linear elastic fracture mechanics (LEFM), the MMB test can be regarded as the superposition of the *double cantilever beam* (DCB) and *end notched flexure* (ENF) tests, respectively used to measure interlaminar fracture resistance under pure fracture modes I and II (ASTM 2013).

We have developed an enhanced beam-theory (EBT) model of the MMB test, wherein the delaminated specimen is schematised as an assemblage of two identical sublaminates partly connected by a deformable interface. The sublaminates are modelled as extensible, flexible, and shear-deformable laminated beams. The interface is regarded as a continuous distribution of linearly elastic–brittle springs, transmitting stresses along both the normal and tangential directions with respect to the interface plane. The model is described by a set of suitable differential equations and boundary conditions. In Bennati et al. 2013a, through the decomposition of the problem into two subproblems related to the symmetric and antisymmetric parts of the loads, an explicit solution for the internal forces, displacements, and interfacial stresses has been deduced. In Bennati et al. 2013b, expressions for the specimen compliance, energy release rate, and mode mixity have also been determined.

Here, following an approach already adopted in Bennati and Valvo (2006) to model buckling-driven delamination growth in fatigue, we analyse the response of the MMB test specimen under cyclic loads. Exploiting the available analytical solution, we apply a fracture mode-dependent fatigue growth law. As a result, the number of cycles needed for a delamination to extend to a given length can be predicted.

Nomenclature

A_1	extensional stiffness of the sublaminates
a	length of the delamination
B	width of the specimen
C_1	shear stiffness of the sublaminates
C	specimen compliance
c	length of the lever arm
D_1	bending stiffness of the sublaminates
E_x	longitudinal Young's modulus
$f, f_\mathrm{I}, f_\mathrm{II},$	factors of fatigue crack law
G	energy release rate
G_c	critical energy release rate
G_I, G_II	mode I and mode II contributions to the energy release rate
G_Ic, G_IIc	pure mode I and mode II critical energy release rates
G_{zx}	transverse shear modulus
H	thickness of the specimen
h	half-thickness of the specimen
k_x, k_z	elastic constants of the tangential and normal distributed springs
L	span of the specimen
ℓ	half-span of the specimen
$m, m_\mathrm{I}, m_\mathrm{II}$	exponents of fatigue crack law
N	number of cycles
P	load applied by the testing machine
P_I, P_II	loads responsible for fracture mode I and mode II
P_d	downward load applied at the mid-span section of the specimen
P_u	upward load applied at the left hand support of the specimen
β	non-dimensional crack length correction for mode mixture
δ	load application point displacement
λ_i	root of the characteristic equation, i = 1, 2 and 5
χ_I, χ_II	crack length correction factors for mode I and mode II
ψ	mode-mixity angle

2. Linear elastic interface model

2.1. Mechanical model

In the MMB test, a laminated specimen with a delamination of length a (Fig. 1b) is simply supported and loaded through a rigid lever (Fig. 1a). We denote with $L = 2\ell$, B, and H the length, width, and thickness of the specimen, respectively. The delamination divides the specimen into two sublaminates, each of thickness $h = H/2$. The load applied by the testing machine, P, is transferred to the specimen as an upward load, P_u, and a downward load, P_d. The lever arm length, c, can be adjusted to vary the intensities of P_u and P_d, thus imposing a desired I/II mixed-mode ratio, G_I/G_{II}. According to ASTM (2013), the downward load, P_d, is applied at the mid-span cross section. Global reference x- and z-axes are fixed, aligned with the specimen longitudinal and transverse directions, respectively.

According to the enhanced beam-theory (EBT) model, the sublaminates may have any stacking sequences, provided that they behave as plane beams and have no shear-extension or bending-extension coupling (Bennati et al. 2013a). In line with classical laminated plate theory (Jones 1999), we denote with A_1, C_1, and D_1 the sublaminate extensional stiffness, shear stiffness, and bending stiffness, respectively. For orthotropic specimens, $A_1 = E_x h$, $C_1 = 5\ G_{zx} h/6$, and $D_1 = E_x h^3/12$, where E_x and G_{zx} are the longitudinal Young's modulus and transverse shear modulus. The sublaminates are partly connected by a deformable interface, regarded as a continuous distribution of linearly elastic–brittle springs. We denote with k_z and k_x the elastic constants of the distributed springs respectively acting along the normal and tangential directions with respect to the interface plane (Fig. 1c).

2.2. Compliance

For a linearly elastic load-deflection response, the specimen compliance is $C = \delta/P$, where P is the applied load and δ is the displacement of the load application point. The compliance of the MMB test specimen turns out to be

$$C_{\mathrm{MMB}} = \left(\frac{3c-\ell}{4\ell}\right)^2 C_{\mathrm{DCB}} + \left(\frac{c+\ell}{\ell}\right)^2 C_{\mathrm{ENF}}, \tag{1}$$

where, according to the EBT model,

$$\begin{aligned} C_{\mathrm{DCB}} &= \frac{2a^3}{3BD_1} + \frac{2a}{BC_1} + \frac{2}{\lambda_1\lambda_2 BD_1}\left[\left(\lambda_1+\lambda_2\right)a^2 + 2a + \frac{1}{\lambda_1} + \frac{1}{\lambda_2}\right] \quad \text{and} \\ C_{\mathrm{ENF}} &= \frac{1}{24B}\frac{A_1h^2}{A_1h^2+4D_1}\left(\frac{a^3}{D_1} + \frac{8\ell^3}{A_1h^2}\right) + \frac{\ell}{4BC_1} + \frac{1}{8BD_1}\frac{A_1h^2}{A_1h^2+4D_1}\frac{1}{\lambda_5^2}\left[\lambda_5 a^2 + a + 2\ell - \frac{2}{\lambda_5} - \frac{4a}{\exp\lambda_5\left(\ell-a\right)}\right] \end{aligned} \tag{2}$$

are the compliances of the DCB and ENF test specimens, respectively, and

$$\lambda_1 = \sqrt{\frac{k_z}{C_1}\left(1+\sqrt{1-\frac{2C_1^2}{k_zD_1}}\right)}, \quad \lambda_2 = \sqrt{\frac{k_z}{C_1}\left(1-\sqrt{1-\frac{2C_1^2}{k_zD_1}}\right)}, \quad \text{and} \quad \lambda_5 = \sqrt{2k_x\left(\frac{1}{A_1}+\frac{h^2}{4D_1}\right)} \tag{3}$$

are the roots of the characteristic equations of the governing differential problem (Bennati et al. 2013b).

Eqs. (2) show that both C_{DCB} and C_{ENF} are the sums of three contributions, respectively depending on the sublaminate bending stiffness (Euler-Bernoulli beam theory), the transverse shear deformability (Timoshenko's beam theory), and the elastic interface. Both C_{DCB} and C_{ENF} are expressed by cubic polynomials of the delamination length, a, except for an exponential term (negligible in most cases) appearing in the expressions for C_{ENF}. Thus, the EBT model provides a rationale for some semi-empirical relationships of the literature (Martin and Hansen 1997).

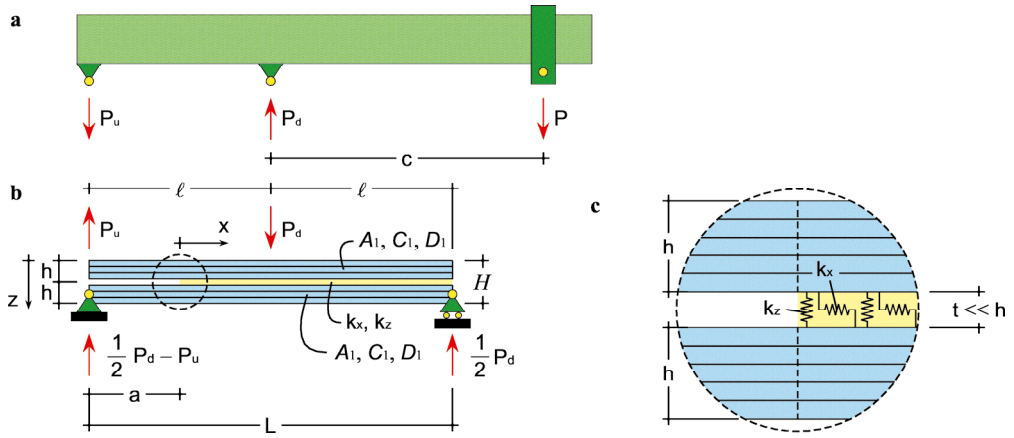

Fig. 1. MMB test: (a) loading lever; (b) laminated specimen; (c) detail of the crack tip region and elastic interface.

Since C_{DCB} depends on k_z (through λ_1 and λ_2) and C_{ENF} depends on k_x (through λ_5), the elastic interface constants can be evaluated experimentally from DCB and ENF tests (Bennati and Valvo 2014). Alternatively, their values may be estimated by establishing an energy equivalence (Valvo et al. 2015), obtaining

$$k_z = \frac{35}{13}\frac{E_z}{2h}, \quad \text{and} \quad k_x = \frac{15}{2}\frac{G_{zx}}{2h}. \tag{4}$$

2.3. Energy release rate

Under I/II mixed-mode fracture conditions, the energy release rate can be written as $G = G_I + G_{II}$, where G_I and G_{II} are the contributions related to fracture modes I and II, respectively. For the MMB test specimen,

$$G_I = \frac{P_I^2}{2B}\frac{dC_{DCB}}{da} \quad \text{and} \quad G_{II} = \frac{P_{II}^2}{2B}\frac{dC_{ENF}}{da}, \tag{5}$$

where

$$P_I = \frac{3c-\ell}{4\ell}P \quad \text{and} \quad P_{II} = \frac{c+\ell}{\ell}P \tag{6}$$

are the loads responsible for fracture modes I and II, respectively. By substituting Eqs. (2) into (5), we obtain

$$G_I = \frac{P_I^2}{B^2 D_1}\left(a+\chi_I h\right)^2 \quad \text{and} \quad G_{II} \cong \frac{P_{II}^2}{16B^2 D_1}\frac{A_1 h^2}{A_1 h^2 + 4D_1}\left(a+\chi_{II} h\right)^2, \tag{7}$$

where

$$\chi_I = \frac{1}{h}\left(\frac{1}{\lambda_1}+\frac{1}{\lambda_2}\right) = \frac{1}{h}\sqrt{\frac{D_1}{C_1}+\sqrt{\frac{2D_1}{k_z}}} \quad \text{and} \quad \chi_{II} = \frac{1}{h}\frac{1}{\lambda_5} = \frac{1}{h}\Bigg/\sqrt{2k_x\left(\frac{1}{A_1}+\frac{h^2}{4D_1}\right)} \tag{8}$$

are crack length correction parameters (Bennati et al. 2013b). Eqs. (8) can be regarded as a generalisation for multidirectional laminates of the formulas given by the ASTM (2013) for unidirectional specimens.

2.4. Mode mixity

To characterise the relative contributions of fracture modes I and II, we introduce the mode-mixity angle,

$$\psi = \arctan\sqrt{\frac{G_{\mathrm{II}}}{G_{\mathrm{I}}}}, \tag{9}$$

which is most conveniently used in fatigue criteria (Kardomateas et al. 1995, Bak et al. 2014). For the MMB test specimen, by substituting Eqs. (6) and (7) into (9) and simplifying, we obtain

$$\psi = \arctan\left[\beta\frac{3c-\ell}{c+\ell}\sqrt{1+4D_1/\left(A_1h^2\right)}\right]^{-1}, \tag{10}$$

where

$$\beta = \frac{a+\chi_1 h}{a+\chi_{\mathrm{II}}h} = \frac{a+1/\lambda_1+1/\lambda_2}{a+1/\lambda_5}. \tag{11}$$

Eq. (10) can be solved with respect to c to obtain the lever arm length corresponding to a desired mode mixity,

$$c = \frac{\beta\sqrt{1+4D_1/\left(A_1h^2\right)}+\cot\psi}{3\beta\sqrt{1+4D_1/\left(A_1h^2\right)}-\cot\psi}\ell. \tag{12}$$

Eq. (12) shows that pure mode I fracture ($\psi = 0°$) would require $c = -\ell$. This corresponds, however, to a negative value of P. Hence, pure mode I tests cannot be performed by using the MMB equipment. Conversely, pure mode II fracture ($\psi = 90°$) is obtained for $c = \ell/3$. Lever arm lengths below such value also result in pure mode II fracture, however with contact and friction between the sublaminates, which may alter the test results.

Figure 2 (a) shows the mode-mixity angle, ψ, as a function of the lever length, c, non-dimensionalised by the half-span of the specimen, ℓ, for three values of β. The blue curve corresponds to the simple beam theory model, where no crack length correction parameter is considered; the orange and red curves correspond to delamination lengths of 50 and 30 mm, respectively. The black dashed line identifies the asymptotic value of the mode-mixity angle, equal to about 18°, which would require an infinite lever arm length, c.

Here, as for the following pictures, the geometrical and mechanical properties (Table 1) correspond to the glass/epoxy specimens tested under static loads by Benzeggagh and Kenane (1996) and fatigue loads by Kenane and Benzeggagh (1997). In particular, the specimens were realised from a quasi-unidirectional 16-ply laminate with 52 vol% of E-glass fibre and M10 epoxy resin (VICOTEX). In fatigue tests, Kenane and Benzeggagh (1997) assumed that the mixed-mode ratios remained constant, while the delamination length increased from 25 to 65 mm. According to the EBT model, as well as for the ASTM (2013), the mode mixity depends indeed on the delamination length, a. Figure 2 (b) shows, however, that this dependence is quite limited in the considered range of a.

Table 1. Geometrical and mechanical properties of the MMB test specimen.

Specimen size	(*mm*)	Elastic constant	(*GPa*)
Span, L	130	Longitudinal Young's modulus, E_x	36.2
Thickness, $2h$	6	Transversal Young's modulus, E_z	10.6
Width, B	20	Shear modulus, G_{zx}	5.6

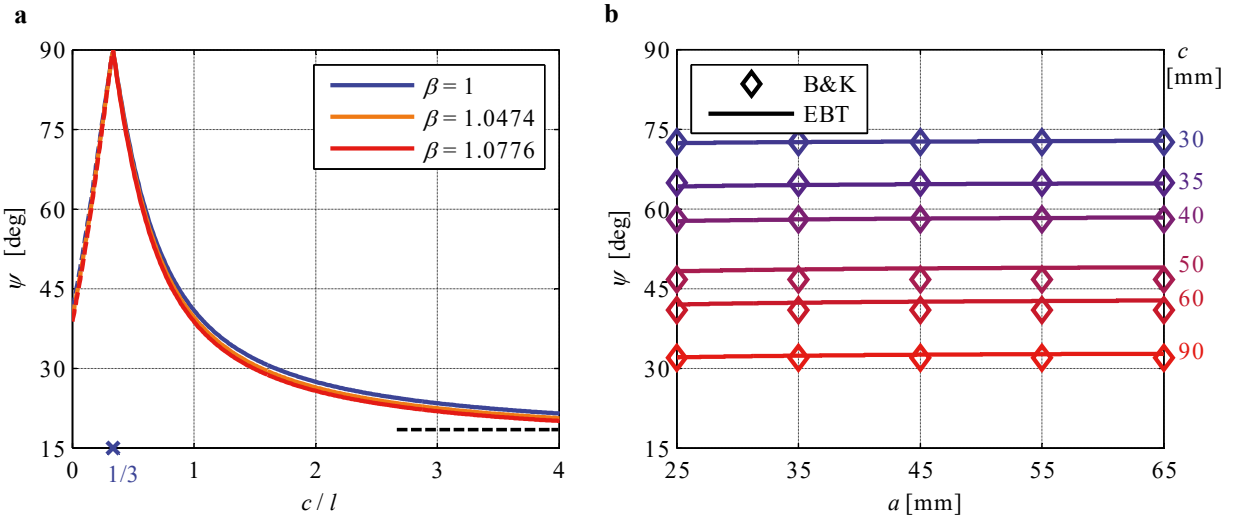

Fig. 2. (a) ψ versus c/ℓ; (b) ψ versus a for the values of c considered by Benzeggagh and Kenane (1996).

3. Delamination growth under quasi-static loads

Under I/II mixed-mode fracture conditions, the critical energy release rate, G_c, equals an intermediate value between those measured in pure modes I, G_{Ic}, and II, G_{IIc}. Many criteria for determining G_c as a function of the mode-mixity are available in the literature. Here, we assume the following elliptical criterion:

$$\left(\frac{G_I}{G_{Ic}}\right)^2+\left(\frac{G_{II}}{G_{IIc}}\right)^2=1. \tag{13}$$

By expressing $G_I = G\cos^2\psi$ and $G_{II} = G\sin^2\psi$, in line with Eq. (9), it can be shown that Eq. (13) is equivalent to

$$G_c(\psi)=\left(\frac{\cos^4\psi}{G_{Ic}^2}+\frac{\sin^4\psi}{G_{IIc}^2}\right)^{-\frac{1}{2}}. \tag{14}$$

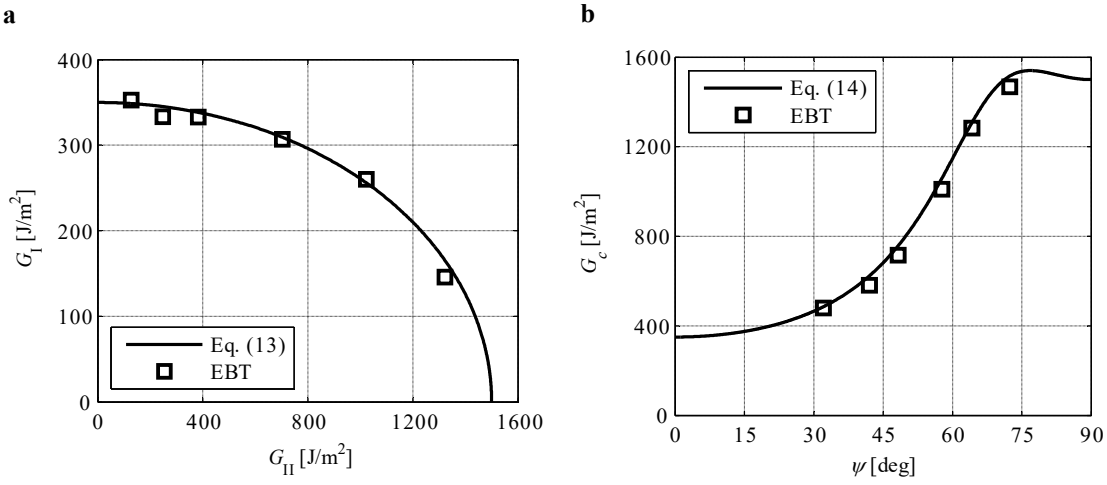

Fig. 3. (a) G_I versus G_{II} at the delamination onset; (b) G_c versus ψ.

Figures 3 (a) and 3 (b) respectively show the elliptical criterion Eq. (13) in the plane of G_I and G_{II} and the critical energy release rate, G_c, as a function of ψ as given by Eq. (14). The plots have been obtained by assuming $G_{Ic} = 350.0$ J/m^2 and $G_{IIc} = 1500.0$ J/m^2. It should be noted that such values do not correspond to those measured in pure mode I and II tests by Benzeggagh and Kenane (1996), but are adopted here because of the good fit with their experimental results for mixed-mode tests, as re-interpreted through the EBT model (the squares in Fig. 3).

Figure 4 shows the theoretical predictions of the EBT model for static tests with different values of c in the plane of the applied load, P, and displacement, δ. For each value of c, an initial linear elastic branch is followed by curvilinear one, which corresponds to static delamination growth. The maximum value of load was obtained as follows. First, ψ is computed from Eq. (10) and G_c from Eq. (14). Then, G_I and G_{II} are determined from Eq. (9) and P from Eqs. (6) and (7). Lastly, the displacement, $\delta = C\,P$, is determined by using Eq. (1). The same procedure was used for the curvilinear branches, whereas the delamination length, a, monotonically increases from 25 to 65 mm.

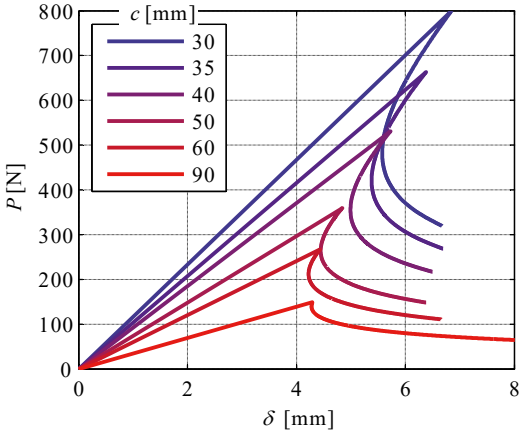

Fig. 4. P versus δ in quasi-static tests (a varying from 25 to 65 mm).

4. Delamination growth under cyclic loads

To illustrate the application of the EBT model to delamination growth under cyclic loads, we consider the MMB fatigue tests on glass/epoxy specimens carried out by Kenane and Benzeggagh (1997). Among the many proposed criteria for fatigue delamination growth (Bak et al. 2014), we choose the law proposed by Kardomateas et al. (1995) for load cycles, where the energy release rate oscillates between G_{min} and G_{max}:

$$\frac{da}{dN} = f(\psi)\frac{\left(\Delta\hat{G}\right)^{m(\psi)}}{1-\hat{G}_{max}}, \tag{15}$$

where N is the number of load cycles performed,

$$\Delta\hat{G} = \frac{G_{max}-G_{min}}{G_c(\psi)} \quad \text{and} \quad \hat{G}_{max} = \frac{G_{max}}{G_c(\psi)}, \tag{16}$$

and $f(\psi)$ and $m(\psi)$ are two mode-dependent parameters. It is assumed that

$$f(\psi) = f_I + (f_{II}-f_I)\sin^2\psi \quad \text{and} \quad m(\psi) = m_I + (m_{II}-m_I)\sin^2\psi, \tag{17}$$

where the parameters f_I, m_I and f_{II}, m_{II} should be determined through pure mode I and II fatigue tests, respectively.

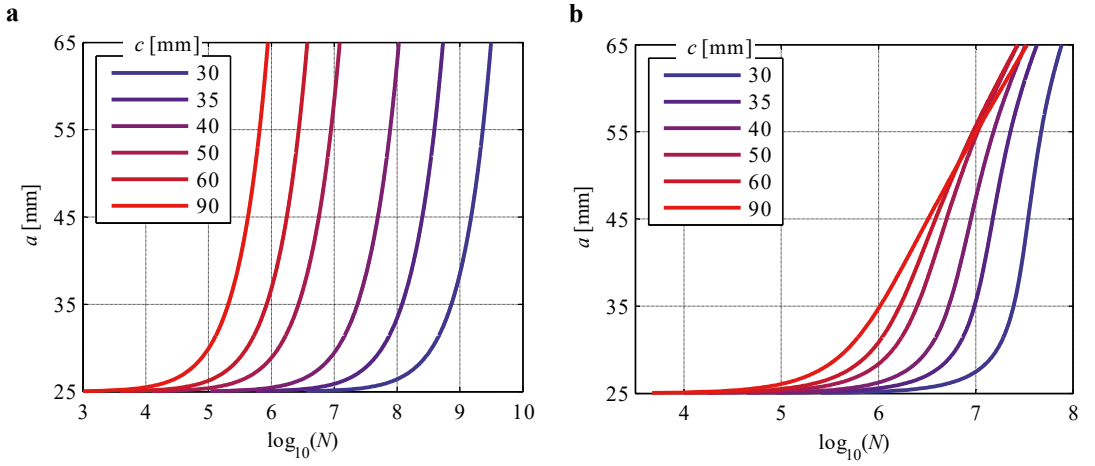

Fig. 5. a versus N for (a) $G_{max} = 200$ J/m^2 and (b) $\delta_{max} = \delta_c/2$, for the values of c considered by Kenane and Benzeggagh (1997).

Figure 5 shows the theoretical predictions of the EBT model for delamination growth under cyclic loads, as obtained by numerical integration of Eq. (15). Curves in figure 5 (a) correspond to load cycles conducted between $G_{\min} = 0$ and $G_{\max} = 200$ J/m^2. Instead, curves in figure 5 (b) have been obtained by supposing that the imposed displacement varies between 0 and one half of the displacement corresponding to the onset of static delamination. From the results of pure mode I and II fatigue tests by Kenane and Benzeggagh (1997), we have calculated the following numerical values: $f_{\mathrm{I}} = 3.37 \times 10^{-4}$ mm/cycles, $m_{\mathrm{I}} = 1.885$, $f_{\mathrm{II}} = 4.9673 \times 10^{-8}$ mm/cycles and $m_{\mathrm{II}} = 4.14$.

5. Conclusions

We have presented an application of the EBT model to describe the MMB test specimen response under static and cyclic loads. The numerical values adopted have to be considered illustrative. For a complete characterisation of materials and validation of the theoretical model, it will be necessary to carry out *ad hoc* experimental tests.

References

ASTM D6671/D6671M-13e1, 2013. Standard Test Method for Mixed Mode I-Mode II Interlaminar Fracture Toughness of Unidirectional Fiber Reinforced Polymer Matrix Composites. ASTM International, West Conshohocken, PA.

Bak, B.L.V., Sarrado, C., Turon, A., Costa, J., 2014. Delamination under fatigue loads in composite laminates: a review on the observed phenomenology and computational methods. Applied Mechanics Reviews 66, 060803.

Bennati, S., Fisicaro, P., Valvo, P.S., 2013 a. An enhanced beam-theory model of the mixed-mode bending (MMB) test – Part I: literature review and mechanical model. Meccanica 48, 443–462.

Bennati, S., Fisicaro, P., Valvo, P.S., 2013 b. An enhanced beam-theory model of the mixed-mode bending (MMB) test – Part II: applications and results. Meccanica 48, 465–484.

Bennati, S., Valvo, P.S., 2006. Delamination growth in composite plates under compressive fatigue loads. Composites Science and Technology 66, 248–254.

Bennati, S., Valvo, P.S., 2014. An experimental compliance calibration strategy for mixed-mode bending tests, Procedia Materials Science 3, 1988-1993.

Benzeggagh, M.L., Kenane, M., 1996. Measurement of mixed-mode delamination fracture toughness of unidirectional glass/epoxy composites with mixed-mode bending apparatus. Composites Science and Technology 56, 439-449.

Jones, R.M., 1999. *Mechanics of composite materials*, 2nd edition. Taylor & Francis Inc., Philadelphia.

Kardomateas, G.A., Pelegri, A.A., Malik, B., 1995. Growth of internal delaminations under cyclic compression in composite plates. Journal of the Mechanics and Physics of Solids 43, 847–868.

Kenane, M., Benzeggagh, M.L., 1997. Mixed-mode delamination fracture toughness of unidirectional glass/epoxy composites under fatigue loading. Composites Science and Technology 57, 597–605.

Martin, R.H., Hansen, P.L., 1997. Experimental compliance calibration for the mixed-mode bending (MMB) specimen. In: Armanios, E.A. (Ed.), *Composite Materials: Fatigue and Fracture* (Sixth Volume), ASTM STP 1285, pp. 305–323.

Valvo, P.S., Sørensen, B.F., Toftegaard, H.L., 2015. Modelling the double cantilever beam test with bending moments by using bilinear discontinuous cohesive laws, ICCM 20 – 20th International Conference on Composite Materials. Copenhagen, Denmark.